electronics

MDPI

Article

A Ka-Band Cylindrical Paneled Reflectarray Antenna

Francesco Greco, Luigi Boccia, Emilio Arnieri * and Giandomenico Amendola

DIMES—Dept. Computer, Modeling, Electronics, and Systems Engineering, University of Calabria, 87036 Rende (CS), Italy; f.greco@dimes.unical.it (F.G.); luigi.boccia@unical.it (L.B.); g.amendola@dimes.unical.it (G.A.)

* Correspondence: emilio.arnieri@unical.it; Tel.: +390984494701

Received: 13 May 2019; Accepted: 3 June 2019; Published: 10 June 2019

Abstract: Cylindrical parabolic reflectors have been widely used in those applications requiring high gain antennas. Their design is dictated by the geometric relation of the parabola, which relate the feed location, *f*, to the radiating aperture, *D*. In this work, the use of reflectarrays is proposed to increase *D* without changing the feed location. In the proposed approach, the reflecting surface is loaded with dielectric panels where the phase of the reflected field is controlled using continuous metal strips of variable widths. This solution is enabled by the cylindrical symmetry and, with respect to rectangular patches or to other discrete antennas, it provides increased gain. The proposed concept has been evaluated by designing a Ka-band antenna operating in the Rx SatCom band (19–21 GHz). A prototype has been designed and the results compared with the ones of a parabolic cylindrical reflector using the same feed architecture. Simulated results have shown how this type of antenna can provide higher gain in comparison to the parabolic counterpart, reaching a radiation efficiency of 65%.

Keywords: reflectarray; Ka-band; reflector antennas

1. Introduction

Reflectarray antennas have been among the most popular research topics of the last decades. The motivations behind this great diffusion are due to the great flexibility of this type of structure that can be indeed designed to meet manifold requirements [1]. Originally, they were introduced as a planar alternative of reflector antennas, advantageously employable in scenarios where the planarity of the reflecting surface could lead to relevant benefits [2]. For example, in space applications the development of inflatable [3] or deployable [4] reflectarrays was widely studied to obtain large reflecting surfaces that can be easily stowed in a small volume during the launch phase. In these cases, the reflecting surface extends outside the satellite main body while the feed is integrated on the spacecraft. This configuration is usually favorable to obtain an optimal illumination of the reflectarray, as the ratio between the geometric size and the focal distance (*f*/*D*) can be large enough to reduce the illumination angle between the feed and the peripherals elements. Typically, reflectarrays are designed with *f*/*D* higher than 0.5, as smaller values determine a great efficiency reduction. As a result, the reflectarray compactness is compromised by the feed location. Although not essential in many applications, this limitation becomes relevant in satellite communications (SatCom) and, in particular, for transportable user terminals. This type of terminal should be easily deployable and transportable with reduced size and light weight. Moreover, the direct integration of the feed with the block up-converter (BUC) and with the low noise block converter (LNB), which are typically too bulky to be incorporated with the reflectarray feed, is of great importance. In view of that, only few examples of SatCom reflectarrays have been investigated so far. For instance, in [5] a transportable reflectarray with dual linear polarization at the Ku-band is presented. This configuration employs a passive sub-reflectarray with an *f*/*D* that exceeds the unity and a main-

reflectarray with 1-bit phase control. An example of a K/Ka SatCom [6,7] reflectarray with *f*/*D* equal to 0.75 is reported in [8], while Tx-only reconfigurable folded reflectarrays are presented in [9,10].

This paper introduces a novel paneled reflectarray configuration that is derived from a parabolic cylindrical reflector. The proposed architecture is conceived for portable K/Ka SatCom user terminals. Cylindrical reflector antennas are limited by the *f*/*D* factor [11–13]. In fact, once height and diameter of the antenna are given, *f*/*D* is fixed and a larger diameter would result in a higher antenna profile. In order to solve this problem and to have a larger aperture without increasing the antenna height, a novel approach is evaluated in which the parabolic reflector is replaced with a segmented reflectarray. The phase of each individual reflectarray element is; thus, adjusted to coherently focus the beam, allowing for a larger aperture without changing the feed position. As a result, the proposed reflectarray leads to a better radiation efficiency while the *f*/*D* can be kept below 0.34.

2. Design Principle

The proposed configuration, shown in Figure 1, is composed by a linearly-polarized feed situated along the *x* axis at a height *f* from the origin. The feed illuminates a reflecting surface having an aperture *D* and *L* along the transversal (*y* axis) and longitudinal (*x* axis) plane, respectively. If the feed structure is symmetric, so is the antenna behavior and each half, shown in Figure 1b, can be independently characterized. The reflecting surface is divided into 2*N* reflectarray panels distributed along a curved surface having cylindrical symmetry. Different strategies can be applied to define the size of the panel in the transversal direction and to choose the surface profile. For the case at hand, the reflecting surface has been obtained, discretizing along the *y* axis a parabola having focus *f*, so that each half of the antenna is composed by *N* panels, namely S_1, …, S_N. The *i*th panel (S_i) has a width W_i and it is composed by a dielectric slab having thickness *h* and relative dielectric permittivity ε_r. The phase of the reflected field has been locally controlled by adjusting the width of M_i strips, which resonate along the antenna E-plane and are extended throughout the entire length of the panels. With respect to a conventional rectangular patch antenna, this approach is preferable because it fully exploits the cylindrical symmetry of the structure, concurring to increase the overall radiation efficiency while preserving the antenna linear polarization. The strips have a periodicity *W* while the width of the *j*th unit cell of the *i*th panel is W_{ij}. As shown in Figure 1a, the electric field radiated by the feed impinges in the *ij* cell with an angle θ_{ij} after traveling a r_{ij} long path. To obtain a beam in the broad side direction, all signals reflected by each cell *ij* must reach the feed with the same phase. This condition is fulfilled if the strip width W_{ij} of the involved cell is chosen to satisfy the following phase condition:

$$-kr_{ij} + \phi_{ij} = 0 \tag{1}$$

where kr_{ij} is the phase shifting related to the distance between the center of the cell and the feed as shown in Figure 1a, *k* is the free space propagation constant and ϕ_{ij} is the phase of the re-irradiated signal from the unit cell evaluated with the Ansys HFSS (2019 R2, ANSYS, Inc, Canonsburg, PA, USA, 2019) [14] model, as shown in Figure 2a.

The dimension of the *i*th segment W_i is derived from the angle θ_i as

$$W_i = \frac{D}{2Ncos(\theta_i)} \tag{2}$$

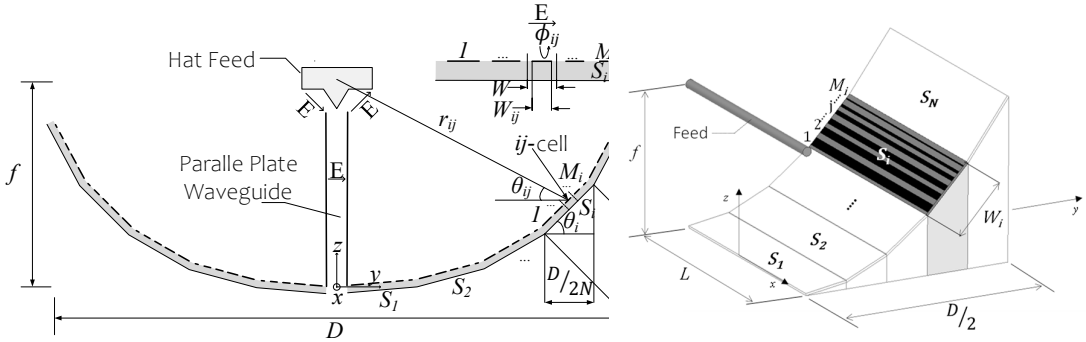

(**a**) (**b**)

Figure 1. Paneled cylindrical reflectarray geometry: (**a**) Section view of the entire geometry; (**b**) 3-D view of half structure.

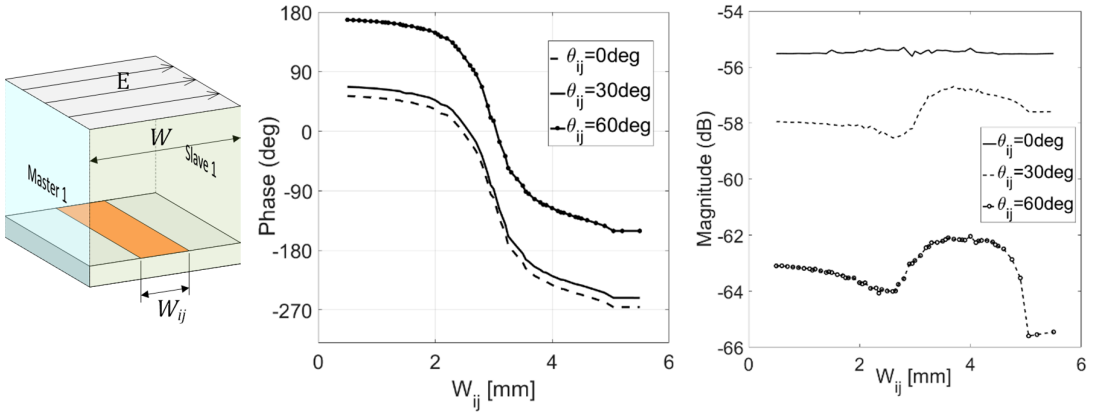

(**a**) (**b**) (**c**)

Figure 2. Single cell characterization at 20 GHz: (**a**) Simulation model of an elementary cell large $W = \lambda/3$ (where λ is computed at 20 GHz); (**b**) phase of the reflected field for different angles of incidence; (**c**) amplitude of the reflected field.

The aperture efficiency of the proposed configuration is related to the dimension of the unit cell W and to the number of segments N. These two parameters can be chosen to maximize the antenna gain, G, defined as [12]

$$G(\theta) = D_F(\theta)\frac{\sum_{i=1}^{2N}\sum_{j=1}^{M_i}|b_{ij}|^2}{\sum_{i=1}^{2N}\sum_{j=1}^{M_i}|a_{ij}|^2}\eta_s \quad (3)$$

where $D_F(\theta)$ is the directivity of the feed, a_{ij} and b_{ij} are the field incident to and reflected by the ij cell, respectively, and η_s is the spillover efficiency. η_s is calculated as the power collected by the array divided by the power radiated by the source. The power collected by the array can be evaluated as described in [13] using the a_{ij} coefficients defined below. The incident and reflected field were evaluated using a finite element method (FEM) tool [14] to simulate the feed and the single strip radiation pattern in the transverse section and assuming a uniform longitudinal distribution. Each strip was characterized using periodic boundary conditions (shown in Figure 2) and using an AD350A (Rogers corp., Chandler, AZ, USA) dielectric slab with a thickness of 0.9822 mm. The field incident to each cell was estimated [13] as

$$a_{ij} = P_{in} \frac{\lambda}{4\pi r_{ij}} e^{-j(2\pi r_{ij}/\lambda)} H_F(\theta_{ij}) H_{El}(\theta) \quad (4)$$

where P_{in} is the total input power, H_F is the hat-feed radiation pattern, H_{El} is the single element radiation pattern, and θ is the direction of radiation. For the case at hand, H_F was modelled as $\cos^2(\theta_{ij})$ and H_{El} was modelled as $\cos(\theta)$. The phase of the field reflected by each cell was evaluated as

$$b_{ij} = a_{ij} S_{11} \quad (5)$$

where S_{11} is the reflection coefficient of each cell simulated using the configuration shown in Figure 2a.

As it can be observed in Figure 2, fixing the inter-element spacing W to $\lambda/3$ (where λ is computed at 20 GHz), the phase of the reflected field can be fully controlled by varying the width of the strip. The relation between the incident and reflected field, evaluated at different angles of incidence $\boldsymbol{\theta}_{ij}$, is then employed to design the reflectarray and to estimate its gain using Equations (1) and (3), respectively.

3. Implementation

The validation of the proposed cylindrical reflectarray was done by taking, as a reference, the parabolic cylindrical reflector proposed in [15]. In this antenna (see Figure 1 in [15]) a parabolic cylindrical reflector was illuminated by a hat-feed placed on its focus. The hat-feed was, in turn, excited through a TEM (transverse electro-magnetic) wave launched by a parallel plate waveguide (PPW), which was located along the reflector longitudinal axis (see Figure 1a). The reference antenna focus, *f*, was equal to 7.5 cm, thus implying an overall aperture *D* equal to 30 cm. The radiating aperture length, *L*, was equal to 40 cm. In this work, the feeding structure of the antenna (hat-feed and PPW) was left unchanged while the cylindrical parabolic reflector was replaced with the proposed paneled reflectarray in order to enlarge the aperture without modifying the overall antenna height. For the case at hand, the cylindrical reflectarray geometry was optimized to operate in the Ka Rx band (19–21 GHz) while the antenna aperture was set to 44 cm, thus making the *f*/D equal to 0.34. It is worth noticing that larger apertures and higher efficiencies could be achieved by redesigning the hat-feed. Although not optimal in terms of illumination efficiency, adapting the feeding structure from another antenna provides a direct comparison with a similar radiating structure while allowing a reduction of the experimental validation costs. Table 1 shows the final dimensions of the segmented reflector calculated with the designing principle described in Section 2; no further optimization stages were needed.

Table 1. Dimensions of the segmented reflector shown in figure 1.

Parameter	Value	Parameter	Value
D	44 cm	M_4	6
f	7.5 cm	M_5	6
L	40 cm	M_6	6
N	7	M_7	7
W	$\lambda/3$	θ_1	2.72°
W_1	3.0462 cm	θ_2	5.11°
W_2	3.0736 cm	θ_3	13.37°
W_3	3.1276 cm	θ_4	18.40°
W_4	3.2069 cm	θ_5	23.16°

W_5	3.3097 cm	θ_6	27.60 deg
W_6	3.4338 cm	θ_7	31.71 deg
W_7	3.5771 cm	-	-

The gain of the proposed structure was numerically evaluated for three different reflectarray configurations: planar, oblique, and paneled. The paneled curvature was defined by a virtual focus $f = 16$ cm. Table 2 reports the gain and radiation efficiency obtained simulating an $L' \times D$ portion of the proposed reflectarray ($L' = 5$ mm) using Equation (3) and a full-wave model [14] (see Figure 3). As it can be seen, the paneled configuration provided higher gain than the planar one due to the possibility to reduce spillover losses. Furthermore, the increased aperture provided higher gain with respect to the cylindrical case, as expected.

Table 2. Gain and efficiency comparison.

Configuration	f (cm)	D (cm)	Gain (dB)	
			Analytical Model	High-Frequency Surface Structure (HFSS)
Parabolic cylindrical reflector	7.5	30	-	18.29
Planar reflectarray	7.5	44	13.6	13.54
Paneled cylindrical reflectarray	7.5	44	19.72	19.69

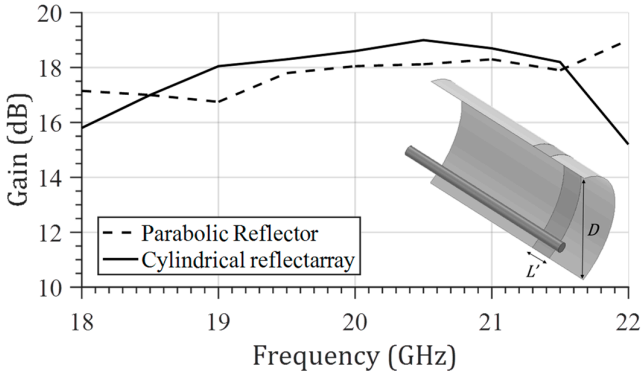

Figure 3. Comparison of the simulated gain performance for a $L' \times D$ portion of the classical parabolic reflector (dotted line) and of the segmented reflectarray (continuous line). $L' = 5$ mm, $D = 30$ cm for the cylindrical parabolic reflector and $D = 44$ mm for the cylindrical reflectarray.

To better understand how the segmented reflectarray works, the electric field amplitude and phase was evaluated along the aperture transversal plane and compared with the ones of the conventional cylindrical reflector presented in [15] (see Figure 4). The two behaviors were similar along the entire aperture but, in the vicinity of the PPW feed, the gaussian vertex employed in the cylindrical reflector generated a smoother amplitude distribution. Furthermore, the phase profile of the reflectarray was less uniform in the vicinity of the border, which would cause a higher side lobe level.

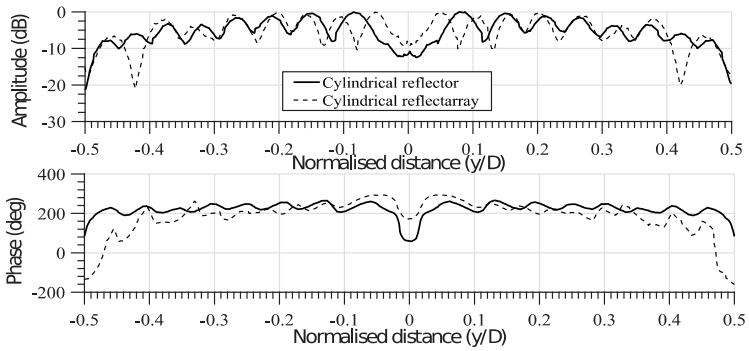

Figure 4. Comparison of field distribution (magnitude and phase) along the aperture of the parabolic cylindrical reflector and of the cylindrical reflectarray.

4. Results and Measurements

As shown in Figure 5, a prototype of the segmented reflectarray was realized. The 14 reflectarray panels (seven on each side of the reflector) were fixed to the feeding structure using two metallic support pairs. Unfortunately, some manufacturing errors occurred in the fabrication of these parts causing discontinuities and misalignment between the dielectric panels 5–7. These discrepancies, not symmetric in the two halves of the antenna, severely affected the radiation pattern as well as the radiation efficiency. In order to evaluate their impact on the antenna performance, a full-wave simulation reflecting the actual geometry of the antenna was performed. Considering that the PPW used in the prototype has an efficiency, e_{PPW}, equal to 0.9, the expected gain of the whole structure could be computed as

$$G_{ex} = 10log_{10}\left(\frac{4\pi L \times D}{\lambda^2} e_{RFA} e_{PPW}\right) \quad (6)$$

where e_{RFA} is the cylindrical reflectarray efficiency. In the nominal case, e_{RFA} is equal to 0.65, thus leading to an expected gain of 37.5 dBi and a radiation efficiency of 58.5%. Full-wave simulations show that in the presence of the gaps and misalignments e_{RFA} was reduced to 25% producing a gain drop of about 4 dB. This value was confirmed by the measurements that showed a gain of about 33 dBi (excluding the losses in the PPW).

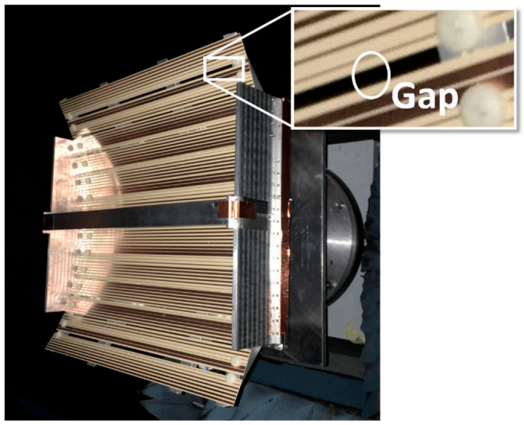

Figure 5. Manufactured segmented reflectarray. The unwanted gap between adjacent segments due to manufacturing errors are also shown.

Figure 6 shows the simulated and measured radiation pattern of the whole structure at the center frequency (20 GHz). As it can be observed, the nominal simulated radiation pattern had a half-power beam width of about 2.8°. The manufacturing errors did not affect this parameter but they caused an

increase of the radiation at low radiation angles as well as an asymmetry. The same figure shows the radiation pattern simulated with the unwanted gaps introduced by the aforementioned manufacturing errors. Good agreement between simulated and measured results were observed.

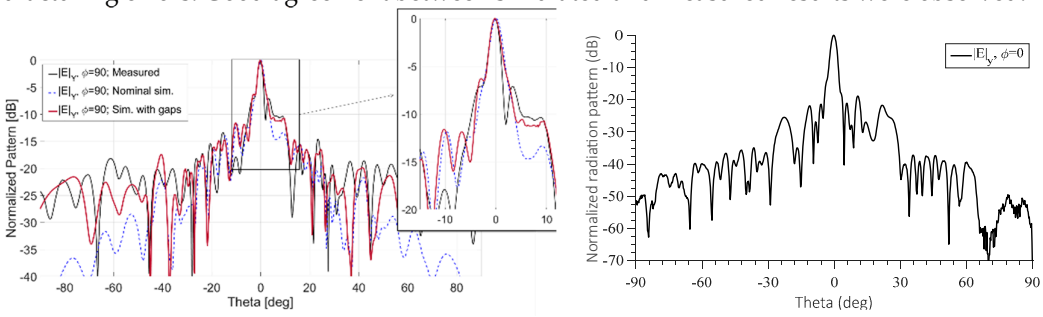

(**a**) (**b**)

Figure 6. Normalized radiation pattern of the proposed configuration at 20 GHz. (**a**) E-plane; (**b**) H-plane (measurement).

The measured gain and reflection coefficient vs. frequency are reported in Figure 7 along with the simulated curves. Simulations took into account the unwanted gaps. As it can be observed, the gain of the reflectarray (including the losses in the PPW) is higher than 31 dBi within the entire Ka Rx band (19–21GHz) while return losses remain below 10 dB over a wider bandwidth. As expected, the gain bandwidth is limited by the narrow band effect of the reflectarray elements.

Measurements was performed in the anechoic chamber of the Laboratorio de Sonido Polytechnic University of Madrid (Spain). The 70 cubic meters chamber has a cutoff frequency of 150 Hz and is ISO 3745 certified. An 18–40 GHz broadband horn antenna with 15 dBi of gain was used during the tests.

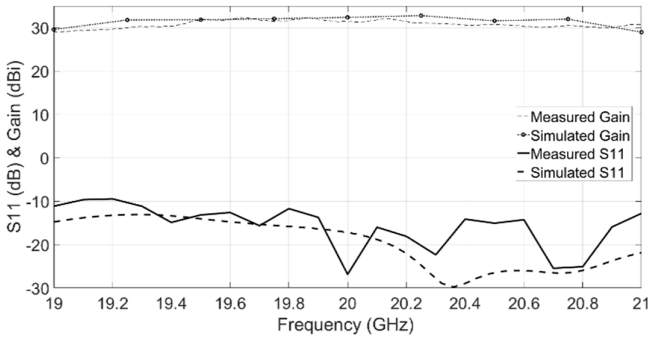

Figure 7. Measured and simulated antenna parameter: gain and matching. Simulations include the gaps shown in Figure 5.

5. Conclusions

This work presents a variant of the reflectarray antennas derived from parabolic cylindrical reflectors. The proposed structure exploits the cylindrical symmetry and the reflectarray properties to increase the radiation aperture without modifying the focus location. As a result, the *f*/*D* factor is reduced from 0.5 to 0.34, whereas in conventional reflectarrays this value is usually chosen to be at least 0.5. Moreover, the use of continuous strips of variable lengths instead of rectangular patches contributes to increase the radiation efficiency. The use of radiating elements along with the curvature of the reflecting surface allows the proposed antenna to have a radiation efficiency of 65%. The proposed configuration can be a valid solution in those applications where large-aperture low-profile antennas should be implemented.

Author Contributions: Conceptualization, G.A. and L.B.; methodology, L.B., E.A.; software, F.G.; validation, F.G.; formal analysis, F.G. and L.B.; investigation, L.B.; resources, E.A.; data curation, G.A.; writing—original draft preparation, E.A.; writing—review and editing, L.B. and E.A.; visualization, F.G.; supervision, G.A.; project administration, G.A.; funding acquisition, G.A.

Funding: This research was funded by TARANTO ECSEL project grant agreement ID 737454.

Acknowledgments: The authors wish to thanks Belèn Galocha, from the Polytechnic University of Madrid (Spain), for her support during the antenna radiation pattern measurements.

Conflicts of Interest: The authors declare no conflicts of interest.

References

1. Huang, J.; Encinar, J.A. *Reflectarray Antennas*; Wiley-IEEE Press: Hoboken, NJ, USA, 2007.
2. Chang, D.C.; Huang, M.C. Multiple-polarization microstrip reflectarray antenna with high efficiency and low cross-polarization. *IEEE Trans. Antennas Propag.* **1995**, *43*, 829–834.
3. Huang, J. The development of inflatable array antennas. *IEEE Antennas Propag. Mag.* **2001**, *43*, 44–50.
4. Hodges, R.E.; Chahat, N.; Hoppe, D.J.; Vacchione, J.D. A Deployable High-Gain Antenna Bound for Mars: Developing a new folded-panel reflectarray for the first CubeSat mission to Mars. *IEEE Antennas Propag. Mag.* **2017**, *59*, 39–49.
5. Montori, S.; Cacciamani, F.; Gatti, R.V.; Sorrentino, R.; Arista, G.; Tienda, C.; Encinar, J.A.; Toso, G. A Transportable Reflectarray Antenna for Satellite Ku-band Emergency Communications. *IEEE Trans. Antennas Propag*. **2015**, *63*, 1393–1407.
6. Arnieri, E.; Boccia, L.; Amendola, G. A Ka-band dual-frequency radiator for array applications. *IEEE Antennas Wirel. Propag. Lett.* **2009**, *8*, 894–897.
7. Amendola, G.; Arnieri, E.; Boccia, L.; Borgia, A.; Focardi, P.; Russo, I. Hybrid waveguide-stripline feeding network for dual polarised arrays at K band. *IET Microw. Antennas Propag*. **2011**, *5*, 1568–1575.
8. Chaloun, T.; Ziegler, V.; Menzel, W. Design of a Dual-Polarized Stacked Patch Antenna for Wide-Angle Scanning Reflectarrays. *IEEE Trans. Antennas Propag.* **2016**, *64*, 3380–3390.
9. Luo, Q.; Gao, S.; Zhang, C.; Zhou, D.; Chaloun, T.; Menzel, W.; Ziegler, V.; Sobhy, M. Design and Analysis of a Reflectarray Using Slot Antenna Elements for Ka-band SatCom. *IEEE Trans. Antennas Propag.* **2015**, *63*, 1365–1374.
10. Smith, T.; Gothelf, U.; Kim, O.S.; Breinbjerg, O. Design, Manufacturing, and Testing of a 20/30-GHz Dual-Band Circularly Polarized Reflectarray Antenna. *IEEE Antennas Wirel. Propag. Lett.* **2013**, *12*, 1480–1483.
11. Tayebi, A.; Gómez, J.; González, I.; Cátedra, F. Broadband design of a low-profile reflector antenna. *IET Microw. Antennas Propag.* **2013**, *7*, 630–634.
12. Clemente, A.; Dussopt, L.; Sauleau, R.; Potier, P.; Pouliguen, P. Focal Distance Reduction of Transmit-Array Antennas Using Multiple Feeds. *IEEE Antennas Wirel. Propag. Lett.* **2012**, *11*, 1311–1314.
13. Yu, A.; Yang, F.; Elsherbeni, A.Z.; Huang, J.; Rahmat-Samii, Y. Aperture efficiency analysis of reflectarray antennas. *Microw. Opt. Technol. Lett.* **2010**, *52*, 364–372. Available online: https://onlinelibrary.wiley.com/doi/abs/10.1002/mop.24949 (accessed on 14 April 2019).
14. High Frequency Surface Structure (HFSS). 2019. Available online: http://www.ansys.com (accessed on 5 May 2019).
15. Greco, F.; Boccia, L.; Arnieri, E.; Amendola, G. K/Ka Band Cylindrical Reflector Antenna for Compact Satellite Earth Terminals. *IEEE Trans. Antennas Propag.* **2019**, in press.